POLITECNICO DI TORINO
Repository ISTITUZIONALE

Modeling and Evaluation of Aircraft Flight Dynamics in Spatially Varying Atmospheric Conditions for Embedded Sensors Calibration

Original
Modeling and Evaluation of Aircraft Flight Dynamics in Spatially Varying Atmospheric Conditions for Embedded Sensors Calibration / Alimhillaj, P., Aimasso, A., Vedova, M.D., Maggiore, P., Poçari, S., Minisci, E.. - (2026), pp. 581-586. (13th IEEE International Workshop on Metrology for AeroSpace, MetroAeroSpace 2026 Madrid (ESP) 01-03 July 2026) [10.1109/metroaerospace69299.2026.11646806].

Availability:
This version is available at: 11583/3016823 since: 2026-10-21T10:25:52Z

Publisher:
Institute of Electrical and Electronics Engineers

Published
DOI:10.1109/metroaerospace69299.2026.11646806

Terms of use:

This article is made available under terms and conditions as specified in the corresponding bibliographic description in the repository

Publisher copyright
IEEE postprint/Author's Accepted Manuscript

©2026 IEEE. Personal use of this material is permitted. Permission from IEEE must be obtained for all other uses, in any current or future media, including reprinting/republishing this material for advertising or promotional purposes, creating new collecting works, for resale or lists, or reuse of any copyrighted component of this work in other works.

(Article begins on next page)

20 November 2026

Modeling and Evaluation of Aircraft Flight Dynamics in Spatially Varying Atmospheric Conditions for Embedded Sensors Calibration

Parid Alimhillaj
dept. of Energy, Meccanical Faculty
Polytechnic University of Tirana
Tirana, Albania
0009-0009-7755-702X

Alessandro Aimasso
dept. of Mechanical and Aerospace Engineering
Polytechnic University of Turin
Turin, Italy
0000-0002-7251-0689

Matteo Dalla Vedova
dept. of Mechanical and Aerospace Engineering
Polytechnic University of Turin
Turin, Italy
0000-0002-3124-2198

Paolo Maggiore
dept. of Mechanical and Aerospace Engineering
Polytechnic University of Turin
Turin, Italy
0000-0003-0218-0730

Spartak Poçari
dept. of Energy, Meccanical Faculty
Polytechnic University of Tirana
Tirana, Albania
0009-0001-2721-4450

Edmondo Minisci
dept. of Mechanical and Aerospace Engineering
Strathclyde Univerisity
Glasgow, UK
0000-0001-9951-8528

***Abstract*— Model-based approaches are increasingly used in aerospace metrology to support the design of measurement strategies and the interpretation of in-flight data under realistic operating conditions. In this context, the availability of reliable flight-dynamics models is essential not only for predicting the aircraft response to atmospheric disturbances, but also for identifying the most informative conditions and locations for sensor deployment. This work investigates the influence of vertical wind gusts on the longitudinal dynamic response of a commercial aircraft through the comparison of two deterministic gust representations: an exponential front, intended to reproduce a smoother and more realistic gust development, and a simplified linear front model with the same characteristic intensity and length. The aircraft response is evaluated by means of a linearized dynamic model implemented in MATLAB/Simulink, and the two gust profiles are compared in terms of load-factor evolution and minimum load factor. The results show that the linear gust model produces a more severe transient response, whereas the exponential profile leads to a smoother and more physically consistent behavior. These findings provide a physics-based basis for the metrological planning of onboard sensing systems, supporting the selection and future positioning of sensors aimed at maximizing the acquisition of informative flight-response data under gust disturbances.**

Keywords*— *Flight Dynamics, Atmospheric Modeling, Aircraft Control Systems, Influence of the Atmosphere on Flight

I. INTRODUCTION

The development of integrated measurement systems that are minimally invasive and capable of providing multiparametric information using the same hardware has gained increasing interest in the aerospace field, particularly for Structural Health Monitoring (SHM), prognostics, and diagnostics applications. In this context, the development of integrated sensor networks capable of ensuring high performance while operating in harsh environments plays a crucial role. These technologies are increasingly investigated within the framework of model-based sensing, where experimental measurements are interpreted through physics-based models in order to provide a more reliable understanding of the monitored system. Fiber optic sensing technology fully meets these requirements thanks to its exceptional physical properties, such as minimal invasiveness, immunity to electromagnetic interference, and multiplexing capability. In recent years, fiber optic sensing systems, such as those based on Rayleigh or Brillouin scattering or on Fiber Bragg Grating (FBG) arrays, have enabled extensive strain measurements along large structural components, including wings and fuselage sections. These technologies provide spatially resolved information on the deformation of the aircraft structure during operation and represent a promising tool for structural health monitoring, in-flight diagnostics and navigation control. However, the interpretation of the large amount of data generated by distributed sensing systems requires reliable physical models capable of describing the aerodynamic disturbances acting on the aircraft and the corresponding dynamic response of the structure. In particular, atmospheric disturbances caused by a non-uniform atmosphere have a significant impact on the aerodynamic forces and moments acting on an aircraft, which depend on its motion relative to the surrounding air. Since the relative velocity between the aircraft and the atmosphere changes when the latter is in motion, the aerodynamic loads must be evaluated with respect to this relative velocity. Among the various atmospheric disturbances encountered during flight, wind gusts represent isolated and clearly identifiable phenomena that can significantly affect aircraft dynamics. Unlike fully developed turbulence, which is usually treated using statistical approaches, gusts can often be represented through deterministic mathematical models describing their velocity field. Such models provide a useful framework for analyzing the aircraft response to atmospheric perturbations and for relating the external aerodynamic excitation to the resulting structural loads. For this reason, the development of suitable mathematical models describing gust disturbances plays an important role not only in flight dynamics analysis but also in supporting the physics-based interpretation of sensing data, enabling a more comprehensive understanding of the interaction between atmospheric phenomena and aircraft structural behavior. In this study, a widely used commercial aircraft configuration is considered, and its dynamic response is analyzed under the influence of a descending gust profile represented by its characteristic mathematical function. The descending gust profile is selected because gusts acting along the vertical axis are generally the

most critical in terms of flight dynamics and aircraft safety [1]. The proposed modeling framework therefore represents a useful reference for linking aerodynamic disturbance models with distributed structural measurements, supporting both the validation of gust response models and the development of advanced aerospace monitoring methodologies.

II. Mathematical Considerations of the Adopted Model

For this study, the aircraft's response to a descending gust has been analyzed. This type of gust can be modeled using the following function:

$$w_g = A_g\left[1 - e^{(-at)}\right] \tag{1.1}$$

This is a continuous time function which schematically represent a realistic gust front. In this way, the parameters of the function are evaluated based on the fact that, after traveling $30\ m$ from the start of the gust front, the aircraft is subjected to 90% of its asymptotic velocity A_g, which is estimated to be around $20\ m/s$. As a result, the minimum load factor (the contingency factor) experienced by the aircraft under these gust conditions is compared with the one obtained from a gradual linear gust that has the same maximum intensity A_g and a front length $H = 30\ m$. To fully define the gust, it is necessary to determine its spatial extent, as well as the linear and angular velocity vectors as follows. [2–6]

$$\bar{V}_g = \begin{Bmatrix} u_g \\ v_g \\ w_g \end{Bmatrix} \tag{1.2}$$

$$\bar{\omega}_g = \begin{Bmatrix} p_g \\ q_g \\ r_g \end{Bmatrix} \tag{1.3}$$

From this, it is possible to express the relative velocities as a function of the absolute velocities in the body axes of the aircraft, denoted as $[V]_B$, and those of the gust, denoted as $[\omega]_g$.

$$\Delta V = \Delta V_B - V_g \tag{1.4}$$

$$\Delta\omega = \Delta\omega_B - \omega_g \tag{1.5}$$

In this case, the analysis is limited to longitudinal motion, for which the linearized equations in the wind axes (Figure 1).are presented in the following equations.

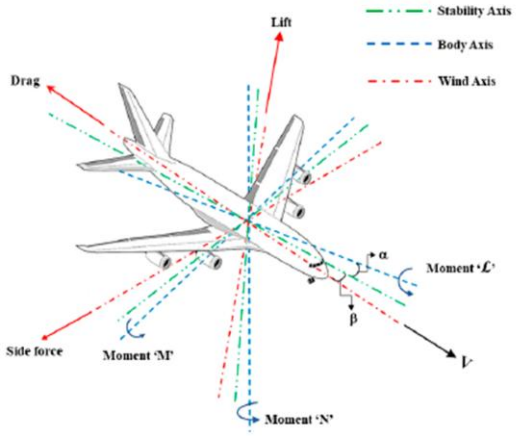


Fig. 1. The stability axes, the body axes of the aircraft, and those of the gust under consideration [9]

$$\Delta\hat{V} = \frac{1}{2\mu}(C_{Tv}cos\alpha_T - C_{Dv})\Delta\hat{V} + \frac{C_{Leq}-C_{D\alpha}}{2\mu}\Delta\alpha - \frac{1}{2\mu}C_{weq}\Delta\theta \tag{1.6}$$

$$\Delta\dot{\hat{\alpha}} = -\frac{(C_{Tv}sin\alpha_T + C_{Lv} + 2C_{weq})}{2\mu + C_{L\alpha}}\Delta\hat{V} - \frac{C_{L\alpha}+C_{Deq}}{2\mu+C_{L\alpha}}\Delta\alpha + \frac{2\mu+C_{Lq}}{2\mu+C_{L\alpha}}\Delta\hat{q} \tag{1.7}$$

$$\Delta\dot{\hat{\theta}} = \Delta\hat{q} \tag{1.8}$$

$$\Delta\dot{\hat{q}} = \frac{1}{\hat{J}_Y}\left[C_{mv} - \frac{C_{m\dot{\alpha}}(C_{Tv}sin\alpha_T + C_{Lv} + 2C_{weq})}{2\mu + C_{L\alpha}}\right]\Delta\hat{V} + \frac{1}{\hat{J}_Y}\left[C_{m\alpha} - \frac{C_{m\dot{\alpha}}(C_{L\alpha}-C_{Deq})}{2\mu+C_{L\alpha}}\right]\Delta\alpha + \frac{1}{\hat{J}_Y}\left[C_{mq} + \frac{C_{m\dot{\alpha}}(2\mu - C_{Lq})}{2\mu+C_{L\alpha}}\right]\Delta\hat{q} \tag{1.9}$$

Here, the velocities refer to the relative ones. If a gust with a linear velocity component is modeled, specifically the vertical component w, and an angular velocity component q, equations (1.6), (1.7), (1.8), and (1.9) can be expressed in terms of these quantities. In particular, for these gust velocities to be included in the equations, they must be nondimensionalized in the form: [7–8]

$$\hat{w}_g = \frac{w_g}{V_{eq}} \tag{1.10}$$

For the angular velocity q, it should be noted that, if the small disturbance hypothesis is applied, this quantity can be easily derived from w, as shown in Figure 2.

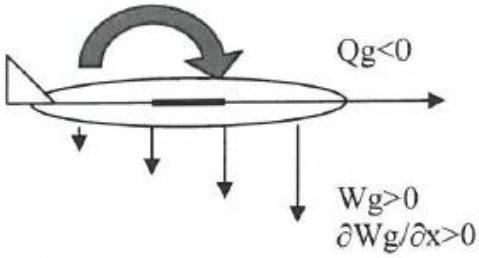


Fig. 2. Schematic representation of small disturbances to determine the angular velocity q

$$q_g = -\frac{\partial w_g}{\partial x} = \frac{\partial w_g/\partial t}{\partial x/\partial t} = -\frac{\dot{w}_g}{V_{eq}} \tag{1.11}$$

$$\hat{q}_g = -\frac{\dot{w}_g}{V_{eq}}t^* \tag{1.12}$$

From which it derives:

$$\Delta\hat{V} = \frac{1}{2\mu}(C_{Tv}cos\alpha_T - C_{Dv})\Delta\hat{V} + \frac{C_{Leq}-C_{D\alpha}}{2\mu}(\Delta\alpha - \alpha_g) - \frac{1}{2\mu}C_{weq}\Delta\theta \tag{1.13}$$

$$\Delta\dot{\hat{\alpha}} = -\frac{(C_{Tv}sin\alpha_T + C_{Lv} + 2C_{weq})}{2\mu + C_{L\alpha}}\Delta\hat{V} - \frac{C_{L\alpha}+C_{Deq}}{2\mu+C_{L\alpha}}(\Delta\alpha - \alpha_g) + \frac{2\mu+C_{Lq}}{2\mu+C_{L\alpha}}(\Delta\hat{q} - \hat{q}_g) \tag{1.14}$$

$$\Delta\dot{\hat{\theta}} = \Delta\hat{q} \tag{1.15}$$

$$\Delta\dot{\hat{q}} = \frac{1}{\hat{J}_Y}\left[C_{mv} - \frac{C_{m\dot{\alpha}}(C_{Tv}sin\alpha_T + C_{Lv} + 2C_{weq})}{2\mu + C_{L\alpha}}\right]\Delta\hat{V} + \frac{1}{\hat{J}_Y}\left[C_{m\alpha} - \frac{C_{m\dot{\alpha}}(C_{L\alpha}-C_{Deq})}{2\mu+C_{L\alpha}}\right](\Delta\alpha - \alpha_g) + \frac{1}{\hat{J}_Y}\left[C_{mq} + \frac{C_{m\dot{\alpha}}(2\mu - C_{Lq})}{2\mu+C_{L\alpha}}\right](\Delta\hat{q} - \hat{q}_g) \tag{1.16}$$

In this case, the effect of the gust on the attitude angle and on the variation of the speed magnitude has been considered negligible, since $\gg W_g$; the only effect of the gust on the velocity vector V is the change in the angle of attack.

By organizing the variables into a vector and writing the system in matrix form, the gust-related variables are grouped into the gust vector U_g, while the corresponding coefficients are placed in the gust matrix B_g.

$$\dot{X} = [A]X + [B_g]U_g \tag{1.17}$$

Where:

$$\dot{X} = \begin{Bmatrix} \Delta\hat{\dot{V}} \\ \Delta\hat{\dot{\alpha}} \\ \Delta\hat{\dot{\theta}} \\ \Delta\hat{\dot{q}} \end{Bmatrix}; X = \begin{Bmatrix} \Delta\hat{V} \\ \Delta\hat{\alpha} \\ \Delta\hat{\theta} \\ \Delta\hat{q} \end{Bmatrix} \; ; \; U_g = \begin{Bmatrix} \hat{w}_g \\ \hat{q}_g \end{Bmatrix} \tag{1.18}$$

$$A = \begin{bmatrix} \frac{1}{2\mu}(C_{Tv}cos\alpha_T - C_{Dv}) & \frac{C_{Leq} - C_{D\alpha}}{2\mu} \\ -\frac{(C_{Tv}sin\alpha_T + C_{Lv} + 2C_{weq})}{2\mu + C_{L\alpha}} & -\frac{C_{L\alpha} + C_{Deq}}{2\mu + C_{L\alpha}} \\ 0 & 0 \\ \frac{1}{\hat{J}_Y}\left[C_{mv} - \frac{C_{m\dot{\alpha}}(C_{Tv}sin\alpha_T + C_{Lv} + 2C_{weq})}{2\mu + C_{L\alpha}}\right] & \frac{1}{\hat{J}_Y}\left[C_{m\alpha} - \frac{C_{m\dot{\alpha}}(C_{L\alpha} - C_{Deq})}{2\mu + C_{L\alpha}}\right] \end{bmatrix}$$

$$\begin{bmatrix} -\frac{1}{2\mu}C_{weq} & 0 \\ 0 & \frac{2\mu + C_{Lq}}{2\mu + C_{L\alpha}} \\ 0 & 1 \\ 0 & \frac{1}{\hat{J}_Y}\left[C_{mq} + \frac{C_{m\dot{\alpha}}(2\mu - C_{Lq})}{2\mu + C_{L\alpha}}\right] \end{bmatrix} \tag{1.19}$$

$$B = \begin{bmatrix} \frac{C_{D\alpha}}{2\mu} & 0 \\ \frac{C_{L\alpha}}{2\mu + C_{L\alpha}} & \frac{C_{Lq}}{2\mu + C_{L\alpha}} \\ -\frac{1}{\hat{J}_Y}\left[C_{m\alpha} - \frac{C_{m\dot{\alpha}}(C_{L\alpha} - C_{Deq})}{2\mu + C_{L\alpha}}\right] & -\frac{1}{\hat{J}_Y}\left[C_{mq} + \frac{C_{m\dot{\alpha}}(2\mu - C_{Lq})}{2\mu + C_{L\alpha}}\right] \end{bmatrix} \tag{1.20}$$

A. Exponential Wind Gust

A descending gust, i.e., a positive one, with a profile that can be modeled by expression (1.1), is considered [5, 10]. In an initial analysis, the aim is to determine the coefficient A_g such that, after traveling 30 meters from the start of the descending gust front, the aircraft is subjected to 90% of the gust's asymptotic velocity A_g, which is 20 m/s.

$$A_g = 20 \tag{1.21}$$

$$0.9 \cdot 20 = 20\left(1 - e^{-a30/V}\right) \tag{1.22}$$

$$t' = 30/V = \frac{30}{800/3.6} = 0.135 \tag{1.23}$$

$$a = 17.0562 \tag{1.24}$$

Examining the quantities in dimensionless form, as follows:

$$\hat{w}_g = \bar{A}_g\left[1 - e^{-\bar{a}\hat{t}}\right] \tag{1.25}$$

With:

$$\bar{A}_g = \frac{A_g}{V} = 0.09$$

$$\bar{a} = a \cdot t^* = 0.18$$

For the angular velocity, its dependence on the linear velocity has already been explained; below, only the definition of its dimensionless form is provided:

$$q_g = -\frac{\dot{w}_g}{V} \tag{1.26}$$

$$\hat{q}_g = -\frac{\dot{w}_g}{V}t^* = -\hat{w}_g \tag{1.27}$$

In summary:

$$\hat{w}_g = 0.09\left(1 - e^{-0.28\hat{t}}\right)$$

$$\hat{q}_g = -0.09 \cdot 0.28e^{-0.28\hat{t}} = -0.01623e^{-0.28\hat{t}}$$

Figure 3 shows the behavior of the two variables.

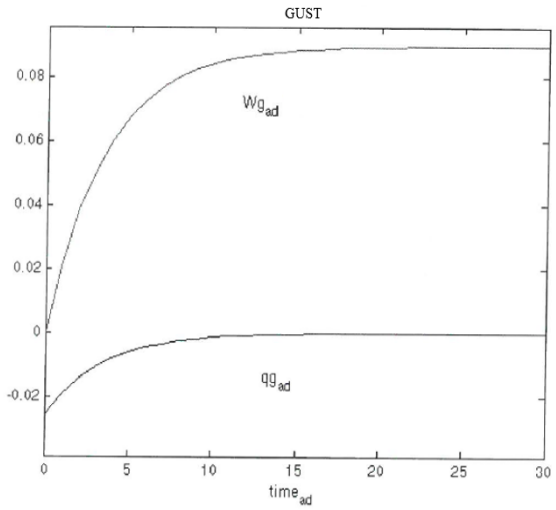


Fig. 3. The time evolution of the two variables, $\hat{w}_g$ (linear velocity) and $\hat{q}_g$ (angular velocity), in the case of an exponential gust.

B. Linear Wind Gust

From the gust calculated using the previous exponential method, the minimum contingency factor generated by the gust must be determined and compared it with that of a gust with a linear front. The linear front model is less realistic than the former, as it does not have a continuous slope; however, it is easier to model because it has an analytical solution for the contingency factor and provides a comparative approximation to the exponential solution.

To understand how valid the approximation of the linear-front gust is compared to more realistic profiles, the following approach is taken:

The linear gust has two known points, one is $t = 0$, where $w_g = 0$, and the point at $t = t'$, where $w_g = A_g$; therefore:

$$\begin{cases} w_g = A_g & 0 < t < t' = \frac{H}{V_0} \\ w_g = A_g & t > t' \end{cases} \tag{1.28}$$

Nondimensionalizing the gust velocity as follows:

$$\begin{cases} \hat{w}_g = A_g\frac{1}{H}t^*\hat{t} & 0 < \hat{t} < \hat{t}' = \frac{H}{V_0} \\ \hat{w}_g = \hat{A}_g & \hat{t} > \hat{t}' \end{cases} \tag{1.29}$$

The angular velocity, now in its dimensionless form, is defined as follow:

$$\begin{cases} \hat{q}_g = A_g \frac{1}{H} t^* & 0 < \hat{t} < \hat{t}' = \frac{H}{V_0} \frac{1}{t^*} \\ \hat{q}_g = 0 & \hat{t} > \hat{t}' \end{cases} \tag{1.30}$$

Figure 4 shows the gust profile modeled using the linear approach.

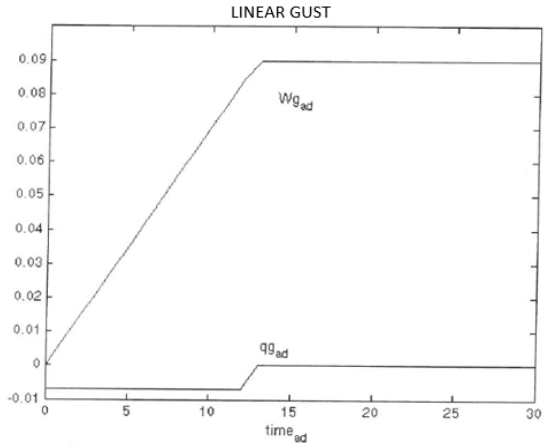


Fig. 4. The time evolution of the two variables, $\hat{w}_g$ (linear velocity) and $\hat{q}_g$ (angular velocity), in the case of a linear gust.

The analytical solution of the contingency factors is obtained by transforming from the time domain to the frequency domain, introducing the gust velocity as input. By multiplying this input with the corresponding transfer function, the output is the 'pitch angle' in the frequency domain. The final step is to convert it back to the time domain. The equation of equilibrium is written as $F = ma$.

$$\frac{1}{2}\rho V^2 S C_{L\alpha}\left(\frac{w_g}{V_0} - \frac{w}{V_0}\right) = \frac{W}{g}\dot{w} \tag{1.31}$$

$$L(w) = W \tag{1.32}$$

$$L\left(\frac{P}{g}\dot{w} + w\frac{1}{2}\rho V S C_{L\alpha}\right) = \left(s\frac{P}{g} + \frac{1}{2}\rho V S C_{L\alpha}\right) W \tag{1.33}$$

$$L\left(w_g \frac{1}{2}\rho V S C_{L\alpha}\right) = \begin{cases} \frac{1}{2}\rho V S C_{L\alpha} A_g \frac{1}{s} & t > t' \\ \frac{1}{2}\rho V S C_{L\alpha} A_g \frac{V}{H}\frac{1}{s^2} & t < t' \end{cases} \tag{1.34}$$

For $t < t'$:

$$W(s) = \frac{\frac{1}{2}\rho V S C_{L\alpha} A_g \frac{V}{H}\frac{1}{s^2}}{s\frac{P}{g} + \frac{1}{2}\rho V S C_{L\alpha}} = \frac{A_g \frac{V}{H} h}{s^3 + s^2 h} = \frac{A_g \frac{V}{H}}{s} - \frac{A_g \frac{V}{H}}{s^2} + \frac{A_g \frac{V}{Hh}}{s+h} \tag{1.35}$$

For $t > t'$:

$$W(s) = \frac{\frac{1}{2}\rho V S C_{L\alpha} A_g \frac{1}{s}}{s\frac{P}{g} + \frac{1}{2}\rho V S C_{L\alpha}} = \frac{A_g h}{s^2 + sh} = \frac{A_g}{s} - \frac{A_g \frac{1}{h}}{s+h} \tag{1.36}$$

By returning to the time domain, it derives:

$$\begin{cases} w(t) = A_g \frac{V^2}{gH}\left(1 - e^{\frac{V}{h}t}\right) \\ w(t) = A_g \frac{V^2}{g}\left(-\frac{e^{-\frac{V}{h}t}}{h}\right) \end{cases} \tag{1.37}$$

From w, based on the small disturbance hypothesis, it is obtained the evolution of the angle of attack.

$$\begin{cases} \alpha(t) = A_g \frac{V}{gH}\left(1 - e^{-\frac{V}{h}t}\right) \\ \alpha(t) = A_g \frac{V^2}{gh}\left(e^{-\frac{V}{h}t}\right) \end{cases} \tag{1.38}$$

Starting from the value of the angle of attack, it is determining the behavior of the contingency factor as:

$$n = \frac{L}{P} = \frac{0.5\rho V^2 S C_{L\alpha}}{P}\alpha = \alpha \frac{1}{2}\rho V^2 C_{L\alpha} \Big/ W/S \tag{1.39}$$

From which:

$$\begin{cases} n(t) = 1 - A_g \frac{V}{gH}\left(1 - e^{-\frac{V}{h}t}\right) \\ n(t) = 1 - A_g \frac{V}{gH}\left(e^{-\frac{V}{h}t}\right) \end{cases} \tag{1.40}$$

III. MATLAB/SIMULINK MODEL AND RESULTS

The Simulink model will take the wind gust as input and output the contingency factor.mThe input consists of: an exponential gust in the first part, and a linear gust in the second part. For the exponential input, two inputs are provided for two velocities, which are calculated based on the time input (clock). These velocities form a vector through the Mux block. For the linear gust, a switch must be added, which determines whether the current time is still within the ramp phase or has entered the constant phase of the wind gust. To implement this, it is sufficient to define the threshold value of the switch and the two inputs between which the appropriate input is selected. In this case as well, it is necessary to input the time, based on which the switch operates. [11–16]

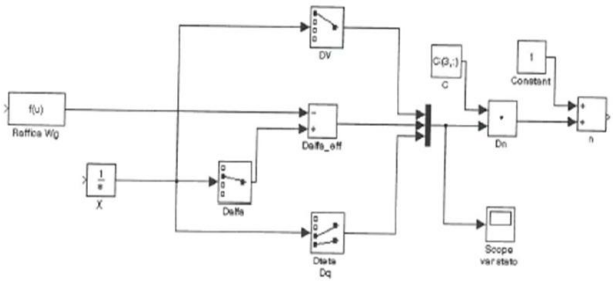


Fig. 5. The MATLAB/Simulink model represents the contingency factors obtained from both types of wind gusts, in order to enable a direct comparison between the two resulting profiles.

In Figure 6, the white line represents the evolution of the contingency factor caused by the exponential gust, while the dark line corresponds to the linear gust. It can be observed that the linear gust causes a contingency factor with a greater absolute minimum value, due to the peak seen in the figure around the value t', which is the moment when the gust presents a discontinuous derivative. The exponential gust, on the other hand, reaches its minimum more gradually, which

nevertheless has a smaller value compared to that produced by the linear gust. The asymptotic behavior is naturally identical, as the aircraft tends to return to its equilibrium state with n = 1. From Figure 7, it can be observed that during the first oscillation from n = -1 to n = 1, the exponential gust is somewhat delayed compared to the linear one, and the maximum value of the load factor is also lower than that obtained with the linear gust. The minimum value of the contingency factor for the two cases are:

n_{min} = -0.666 for the exponential gust

n_{min} = -0.782 for the linear gust

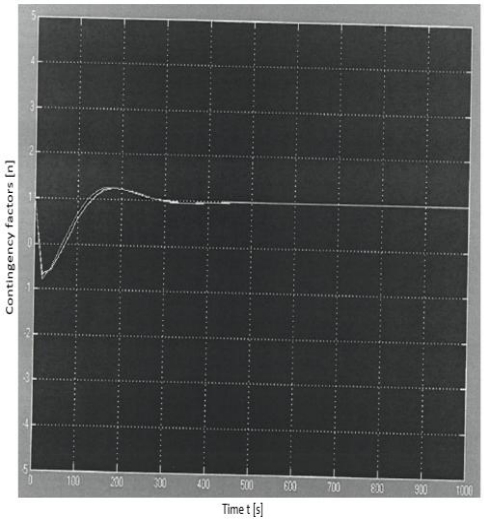


Fig. 6. The contingency factor, obtained from both types of wind gusts — the light one from the exponential gust and the dark one from the linear gust.

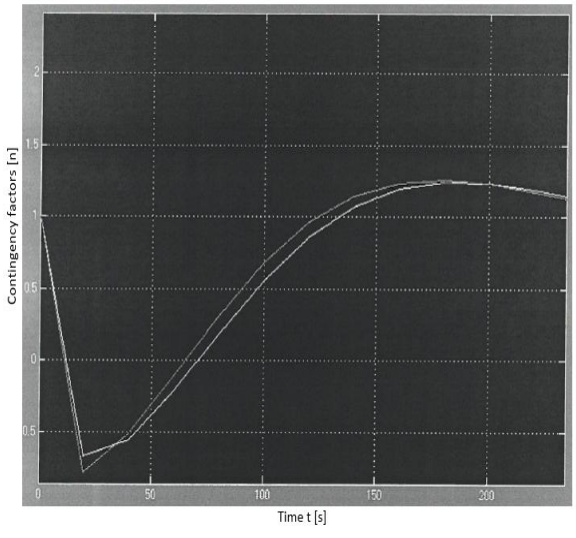


Fig. 7. Detail of the "maximum" contingency factor graph, obtained from both types of wind gusts — the white line from the exponential gust and the dark line from the linear gust.

Table I. Data of the model

$W = 45\,360\ kg$	[1]	Weight of the aircraft
$S = 154.7\ m^2$	[2]	Wing area
$c = 4.7\ m$	[3]	Aerodynamic chord
$ea = 7$	[4]	Static margin with fixed control
$X_G/c = 0.35$	[5]	Normalized position of the center of gravity (CG)
$X_N/c = 0.50$	[6]	Normalized position of the neutral point
$\alpha_T = 0$	[7]	Angle of incidence of the horizontal stabilizer
$C_D = 0.016 + C_L^2/\pi eA$	[8]	Drag polar equation Where: *0.016* — Parasite drag (constant) $C_L^2/\pi eA$ — Induced drag caused by lift C_L— Lift coefficient π — Mathematical constant pi (≈ 3.1416) e — Oswald efficiency factor (typically between 0.7 and 0.95); the closer to 1, the more efficient the wing. A — Wing aspect ratio $A = \frac{b^2}{S}$ where b is wingspan and S is wing area
$C_{L\alpha} \cong 0$	[9]	Lift coefficient does not vary with changes in the angle of attack (α)
$C_{M\alpha} \cong -4.2$	[10]	Derivative of the aerodynamic pitching moment coefficient with respect to the angle of attack α. A negative value (in this case, -4.2) indicates that the moment acts in a stabilizing direction.
$C_{Lq} \cong 0$	[11]	Derivative of the lift coefficient C_L with respect to pitch rate q (angular velocity in pitch). A value of 0 means that changes in q do not affect lift.
$C_{Mq} = -22.9$	[12]	Derivative of the aerodynamic pitching moment coefficient with respect to pitch rate q . The negative value (−22.9) indicates a strong restoring moment that stabilizes the aircraft in pitch.
$\hat{J}_y = 7\mu$	[13]	Non-dimensional moment of inertia about the *y*-axis (lateral axis of the aircraft). μ is a non-dimensional mass parameter used to normalize the equations of motion. It is defined as:

$$\mu = \frac{2m}{\rho S c}$$

where:

- m = mass of the aircraft
- ρ = air density
- S = wing area
- c = mean aerodynamic chord

Thus, 7μ means that the moment of inertia of the aircraft is seven times the normalized mass parameter for lateral motion.

IV. Conclusions

The present study has shown that the choice of gust model significantly affects the predicted longitudinal response of the aircraft, with the linear gust leading to more conservative transient loads and the exponential gust providing a smoother and more realistic representation of the disturbance. Beyond its relevance for flight-dynamics analysis, this modelling framework is intended as the first step toward a metrology-oriented methodology for onboard measurement planning. In particular, the numerical model can be used to identify the flight variables, response regions, and operating conditions that are most sensitive to gust excitation, thereby supporting the optimal positioning and selection of sensors for enhanced data acquisition. At the current stage, the work focuses on the flight-dynamics modelling aspect. For the conference presentation, the current flight-dynamics framework will be complemented by a preliminary sensor-placement analysis aimed at assessing how the model can support measurement planning and data acquisition effectiveness.

References

[1] P. Gili, M. Battipede., Appunti Dinamica e Controllo del Velivolo, Politecnico di Torino, Anno Academico 2004.

[2] A. Bacciotti., Teoria Matematica dei Controlli,. CELID editor, Torino 1998.

[3] L. Amerio., Analisi Matematica Volume III - 1-2,. UTET, Torino 1989

[4] C. Bisi, R. Fioresi,. Metodi matematici per le scienze applicate. CEA Casa Editrice Ambrosiana, 2022.

[5] J. Roscam,. Airplane Flight Dynamics & Automatic Flight Controls: Part I/II., DARcorporation, 1998.

[6] B. Etkin,. Dynamics of Atmospheric Flight., Dover Publication INC, 1972.

[7] B. L. Stevens, E. N. Johnson, and F. L. Lewis., Aircraft Control and Simulation: Dynamics, Controls Design, and Autonomous Systems., Wiley, 2010.

[8] R. C. Nelson., Flight Stability and Automatic Control., WCB/McGraw-Hill, 1998.

[9] K. Mehmood, S. Ali Shah, T. Amin Khan, T. Ali Shams, D. Kukulka., Flight Dynamic Characteristics of Wide-Body Aircraft with Wind Gust and Turbulence., Fluids 2023, 8, 320. https://doi.org/ 10.3390/fluids8120320.

[10] Irving, J.P. Robust Flight Control in a Computational Aircraft Control Engineering Environment. Garteur FM(AG08)/TP-088-2. 1995. Available online: https://garteur.org/wp-content/reports/FM/FM_AG-08_TP-088-2.pdf (accessed on 26 August 2020).

[11] P.Alimhillaj, A. Londo, M. D. L. Dalla Vedova - Behavior analysis of fluid dynamic instabilities in aerospace servovalves numerical models, 2nd International Conference "Engineering and Entrepreneurship" Proceedings (ICEE-2019), UPT Tirana, Albania October 2019.

[12] M. D. L. Dalla Vedova, P. Alimhillaj – Study of New Fluid Dynamic Nonlinear Servovalve Numerical Models for Aerospace Applications, 2nd European Conference on Electrical Engineering & Computer Science 20 – 22 December 2018, Bern, Switzerland.

[13] P. Alimhillaj, M. Alcani, M. D. L. Dalla Vedova, L. Lamani, S. Pocari – Coulomb Friction Model Analysis, Acting on an Aerospace Servocommand. Proceedings of the Joint International Conference: 10th Textile Conference and 4th Conference on Engineering and Entrepreneurship 19 – 20 October, Tirana, Albania, Springer 2024, pp. 197-210.

[14] A. Dorri, S. Poçari, A. Londo, P. Alimhillaj - PID Control for Pneumatic Cylinder Stiffness for Aerospace Applications. International Journal of Mechanics and Control, ISSN: 1590-8844, Vol. 24, No. 01, 2023.

[15] M. D. L. Dalla Vedova, P. C. Berri, C. Corsi and P. Alimhillaj - New synthetic fluid dynamic model for aerospace four-ways servovalve, International Journal of Mechanics and Control (JoMaC), ISSN: 1590 8844, December 2019.

[16] P. Alimhillaj, E. Minisci, M. D.L. DallaVedova, A. Dorri - Analogies Between Simple Mechanical Systems and Electrohydraulic and Electromechanical Servomechanism. International Journal of Mechanics and Control, ISSN: 1590-8844, Vol. 25, No. 01, 2024.